SELECTIVE LASER MELTING OF INCONEL 625 USING PULSE SHAPING

K. A. Mumtaz, N. Hopkinson, Rapid Manufacturing Research Group, Loughborough University, Leicestershire, LE11 3TU, UK

Abstract **Reviewed, submitted September 10, 2008**

Pulse shaping is a technique used to temporally distribute energy within a single laser pulse. This allows the user to have an added degree of control over the heat delivered to the laser material interaction zone. Pulses that induce a gradual heating or a prolonged cooling effect can be generated with peak power/pulse energy combinations specifically tailored to control melt pool properties and eventual part formation. This investigation used a pulsed 550W Nd:YAG laser to melt 0.1mm layers of Inconel 625 from a powder bed. Initially a set of optimization experiments were completed to develop laser parameters that enabled the production of thin wall parts with low top and side surface roughness. Thin wall parts were then built using pulse shape control employing a variety of pulse energy distributions. Parts built with and without pulse shape control were measured for width, top and side surface roughness. The effectiveness of pulse shaping control is discussed including potential benefits for use within Selective Laser Melting (SLM).

1 Introduction

Industry is become increasingly interested in Solid Freeform Fabrication (SFF) technologies to produce fully functional metal parts. This family of processes involves a layer-wise shaping and consolidation of material (e.g. powder, wire) allowing parts to be produced with a high geometric freedom directly from a CAD model. The use of SFF has also the potential to drastically reduce the time period between the initial conceptual design of a part and its actual fabrication. A group of SFF technologies known as Direct Metal Laser Fabrication (DMLF) utilize lasers to consolidate metal. One such DMLF process known as Selective Laser Melting (SLM) builds metal parts by melting powder from a powder bed using a laser.

1.1 Selective Laser Melting

SLM is a powder bed process that begins with the deposition of a thin layer of powder onto a substrate. A high power laser raster scans the surface of the powder, the heat generated causes powder particles to melt and form a melt pool [Santos *et al.* 2004]. Once the layer has been scanned another layer of powder is deposited and is again melted by the laser. Figure 1 shows a schematic of this process. Powder particles that are not melted remain loose and are removed once the component is complete. Supports are required to anchor down certain unsupported features due to shrinkage and curling of solidifying material. This restricts the processes geometric freedom and incurs further post processing operations to remove supports.

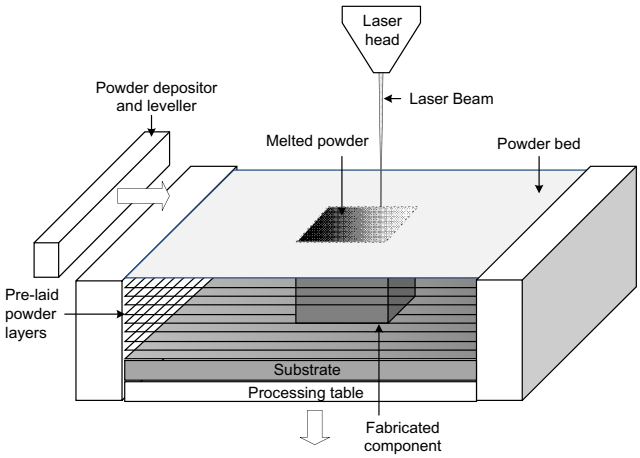

Figure 1 Selective laser melting process

The SLM process has great potential within the manufacturing of specialised functional applications. Schwendner *et al.* believe DMLF processes such as SLM are the most viable technologies for the direct fabrication of complex metallic components [Schwendner *et al.* 2001]. This is due to the versatility, accuracy and small spot size (S_d) of a laser beam. The small spot size reduces the melt width enabling the production of high resolution parts. The main advantage of freeform fabrication processes such as SLM is the capability to build complex geometries that would be otherwise difficult to produce using conventional manufacturing processes. The possibility to build thin wall parts to a high resolution complements the technology's main advantage and extends its manufacturing capabilities.

Direct processing using SLM is not without its difficulties and constraints. SLM issues mainly revolve around the use of high powered lasers to produce high temperatures capable of completely melting the powder. High heat input often causes an increase in material vaporization and spatter generation during processing. Surface roughness is another SLM issue that is influenced by particle melting and re-solidifying mechanisms.

1.2 Surface Roughness and Part Resolution

The surface roughness of a part is critical in many applications with some applications requiring a surface roughness of 0.8μm or better to avoid premature failure from surface initiated cracking [Dalgarno 2007]. Commercial powder bed machines such as MCP's Realizer, EOS M270 etc. often require post processing operations such as surface machining, polishing and shot peening to attain final part surface finish.

The top R_a of a solidified melt pool can be affected by a rippling effect that occurs due to surface tension forces exerting a shear force on the liquid surface. This is primarily due to a surface temperature difference between the laser beam and the solidifying zone caused by the motion of the laser beam. As the thermal gradients reduce, gravity and surface curvature counteract this external shear forces and would eventually restore the surface height of the melt pool to the free level [Ramos *et al.* 2003]. However, viscous forces delay this relaxation process, quick melt pool solidification time often ensures that complete relaxation is not fully achieved.

Investigations using pulsed lasers have reported that top R_a can be reduced using a high laser spot overlap (S_{ov}), achieved at low scan speeds (V) and high repetition rates (f) (see Figure 2) due to melt pool stabilization and reduced surface profile variation on top of the solidified melt pool [Niu *et al.* 1998; Fischer *et al.* 2003]. However low scan speeds and high repetition rates can significantly increase the volume of liquid within the melt pool and promote a phenomenon known as balling. Balling is the breakup of the melt pool into small spheres. It occurs when molten material does not wet well to the underlying substrate or material due to high surface tension differences generated as a result of variations in thermal properties across the melt pool [Fuh *et al.* 1995; Kruth *et al.* 2003; Morgan *et al.* 2004]. These thermal gradients cause a thermocapillary flow of a fluid within the melt pool from regions with low surface tension to regions with high surface tension, known as Marangoni convection [Rombouts *et al.* 2006]. The breaking up of the melt pool into smaller entities reduces the variation in melt pool surface tension. Balling can increase with the generation of excessive molten material or if too low viscosity exists within a melt pool [Agarwala *et al.* 1995]. Kruth *et al.* stated that when the total surface of a molten pool becomes larger than that of a sphere with the same volume, the balling effect takes place [Kruth *et al.* 2004]. Balling is a severe impediment on interlayer connection, it decreases part density and increases top/side R_a. However the balling effect more dominantly affects the side R_a of parts due to the direction of balling scattering to either side of the melt pool rather than settling on the top surface.

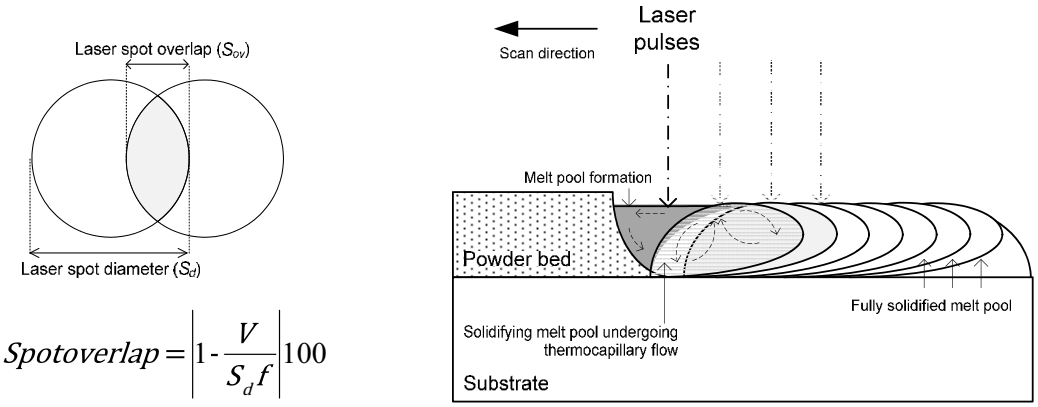

Figure 2 Laser spot overlap and formation of melt pool using a pulsed laser

The achievable minimum feature size (resolution) has great influence on part accuracy. The dimensional tolerances and repeatability are key factors with any DMLF technology. The minimum resolution is of high importance in design of functional parts e.g. for thin walls or open cell structures in medical applications. Thin walls are an example for so-called positive minimum feature size (smallest solid part possible) while open cells are an example for negative minimum feature size (smallest gap size possible) [Rehme *et al.* 2005].

Material vaporization during processing, surface roughness and part resolution are all heavily dependent on laser processing parameters and melt pool control. A technique known as pulse shaping has been shown to extend the degree of control over a laser's energy distribution and therefore has the potential to improve the control over melt pool formation, stability and eventual part properties.

1.3 Pulse Shaping

A pulsed laser emits bursts of energy that consist of a fixed amount of energy for a specified duration. Pulse shaping is a technique used to temporally distribute energy within a single laser pulse. It can also be defined as a variation in power supplied to a laser to change the shape of the output pulse and subsequently the heat distribution within the pulse [Kanzler 2006]. Changing the energy distribution within a pulse can completely change the melting behaviour of a material. Pulse shaping can be accomplished by dividing the pulse's current used to excite a laser's flash lamp into as many as 20 individual sectors and specifying the duration and peak power of each sector. The current supplied by the electric power supply causes the flashlamps to emit light that is absorbed and amplified by the Nd:YAG crystal (only for Nd:YAG laser). This amplified light is emitted in short bursts/pulses through various focusing lenses and eventually onto a work piece as shown Figure 3 (a). Electric power supply is therefore one of the main factors that dictate the characteristics of the laser pulse. This allows the user to specifically tailor the energy distribution to the nearest 0.5ms within a single laser pulse. The electric power supply is set using a Hgt control ranging from 0-100%, 0% indicates no current and 100% indicates maximum current. Figure 3 (b) shows an example of a standard pulse's demand profile. This is known as a rectangular pulse shape or "top hat" pulse shape with power densities remaining nominally constant throughout the pulse. Rectangular pulse shapes are the simplest and most extensively used laser pulse shape within academia and industry containing only one energy sector. This pulse shape is fed to the flashlamps but due to the filter effect a more realistic output profile of the laser is represented in Figure 3 (c). With most solid state lasers such as the Nd:YAG, the use of a rectangular pulse shape input creates an overshoot that can be between 75-100% over the allocated average peak power (P_{pav}) for the first 0.7-1.1ms and comprises of 2-5% of the pulse energy [Bransch *et al.* 1994]. The extent of the overshoot varies according to the laser parameters. This overshoot can be beneficial in regards to increased penetration in laser drilling [Cheng *et al.* 2000], however an over usage of energy within a very short space of time can increase material spattering [Petrov *et al.* 1992]. After the overshoot the laser power delivery normalizes to its steady state value for the majority of the pulses duration. This is then followed by an abrupt loss of power that results in rapid cooling of the processed material. The standard pulse shape's laser output will characteristically remain the same even with use of varied pulse durations and pulse energies.

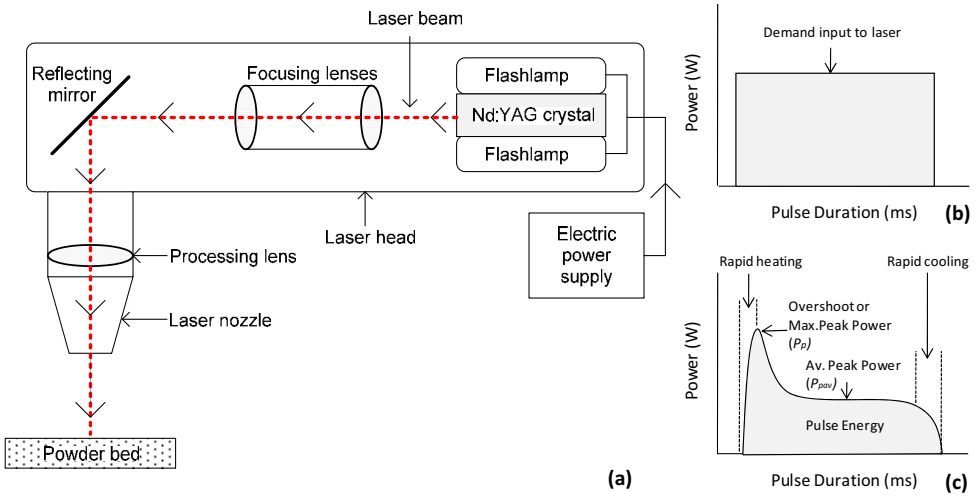

Figure 3 Pulse shape generation (a), laser input demand (b) & laser output (c)

Pulse shaping research has mainly focused on the use of two pulse shapes, ramp up and ramp down. Figure 4 (a) and (b) shows the demand input and output of a ramp up and ramp down pulse shape. As the names suggest these pulses either emit the majority of their power early or late within the pulse. This equates to either a gradual heating or gradual cooling of material. However pulse shapes can be adjusted such that a very complex heating distribution is applied, as shown in Figure 4 (c). The range of useable peak power/pulse energy combinations at a fixed pulse duration can be extended allowing a further improved control over laser processing.

Within the laser welding of metal sheet studies have shown that altering the laser current input demand and producing alterative pulse shapes are beneficial in reducing spatter generation, porosity formation, hot cracking and improvement of weld surface finish [Weedon 1987; Badawi *et al.* 1989; Petrov *et al.* 1992; Katayama *et al.* 1993; Bransch *et al.* 1994].

Very limited work to date has been conducted using pulse shaping techniques to laser process metal powder. Sparks *et al.* used a 1kW CO_2 diode laser to melt powder fed H13 tool steel [Sparks *et al.* 2006]. From preliminary studies it was found that varying the duration of a ramp down pulse shape influenced microstructure grain growth and could potentially improve properties such as part hardness or fatigue strength.

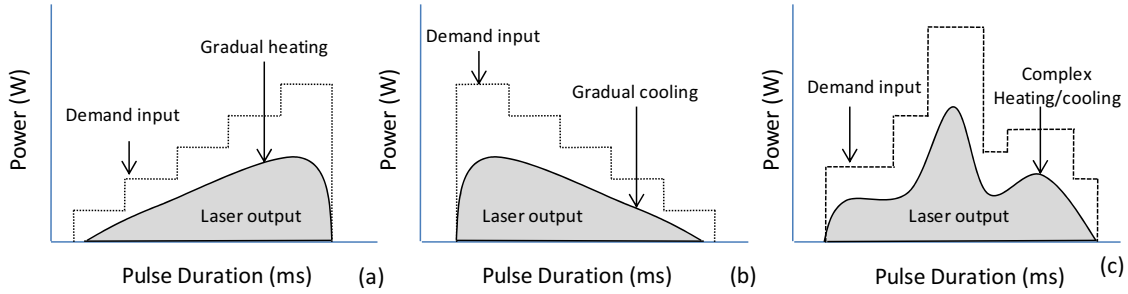

Figure 4 Ramp up (a), ramp down (b) and complex (c) pulse shapes

2 Experimental Methodology and Testing

A set of optimization experiments were initially carried out to identify a set of processing parameters that produced thin wall parts with low top/side R_a. Using these optimum parameters pulse shaping techniques were employed to produce ramp up and ramp down pulse shapes. Their effects on part top/side R and width were tested. The degree of plasma plume generated during processing was also measured during processing to identify a link between the use of certain pulse shapes and amount of spatter generation.

2.1 System Setup

The SLM system used within this investigation included a GSI Lumonics JK701H Nd:YAG laser. The laser has a TEM_{00} Gaussian profile, a spot size of 0.8mm and a maximum power output of 550 W. The pulses of laser energy generated by the flash lamps are fed through a 1mm Ø silica optical fibre delivery cable to the laser head and are deflected through 90° by a reflecting mirror onto a focusing optic. The light is focused and passes through the laser nozzle onto the powder bed. Powder is deposited onto a steel substrate that is itself placed on a processing table that is driven by a 4-axis CNC controlled machine.

Argon gas is fed through the laser nozzle onto the processing area at a rate of 10ml/s to protect the parts from the effects of oxidization. Pulse shape monitoring was undertaken using an externally fitted digital storage PC oscilloscope (PicoScope 3205) to measure and analyse voltage waveforms.

2.2 Material Characterization

Inconel 625 powder (Sandvik Osprey, UK) was supplied sized to $53 \pm 25\mu m$. The exact particle size distribution was measured to be a D(v,0.1) of 22.51μm (10% of the volume distribution is below this value), D(v,0.5) of 45.48μm (volume median diameter, 50% of the distribution is above and 50% is below this value) and a D(v,0.9) of 58.59μm (90% of the volume distribution is below this value).

3 Initial Optimization

Experiments were initially conducted to identify laser process parameters that without pulse shaping techniques would produce thin wall parts with minimum a top and side surface roughness.

3.1 Parameters and Testing

Samples 25mm in length were processed from four powder layers each with a thickness of 100μm. Initially variable pulse energy, repetition rate and scan speed parameters were used, as shown in Table 1. The maximum useable repetition rate used within processing was restricted with the use of higher pulse energies. This was done in order to reduce excessive spatter generation due to the increase in energy density when using higher pulse energies. The shortest pulse duration of 0.5ms was used throughout optimization experiments as it would assist the fabrication of thinner parts due to a reduced volume of liquid being produced within the melt pool due to shorter laser on time [Mumtaz *et al.* 2008].

Pulse Width (ms)	Pulse Energy (J)	Repetition Rate (Hz)	Scan Speed (mm/m)
0.5	0.5	30-100	100- 400
0.5	0.6	30-70	100- 400
0.5	0.7	30-50	100- 400

Table 1 Parameters used within initial optimization experiments

Sample top/side R_a was measured using a Talysurf CLI 2000. The Talysurf evaluated 12.5mm of the samples surface, a cut-off length of 2.5mm was used to determine the arithmetic average roughness (R_a). Sample width was measured using digital callipers. During processing plasma plume height was measured using a fixed digital video camera and computer software ImageTool. A plasma plume is ionized metal vapour that can exert a recoil pressure on the melt pool. Increases in plasma plume intensity are directly related to increases in spatter ejection [Park *et al.* 1999] leading to powder bed contamination and obstruction of powder depositor/leveller.

3.2 Optimization Results

Higher laser spot overlaps formed at lower scan speeds and high repetition rates reduced top R_a as shown in Figure 5(a). Percentage overlaps above 90% tended to reduce the top R_a of samples. This is related to the spherical masses produced by the laser pulses coming nearer together reducing the variation in surface profile. It is believed that the use of slower scan speeds gives more time for molten material to flow and smoothen out the top surface profile due to gravity and surface curvature [Ramos *et al.* 2003], however this may also be related to the fact that higher spot overlaps are more easily generated at lower scan speeds, therefore reducing variation in surface profile.

Figure 5(a) also shows that spot overlap increases the side R_a of samples increased. Higher spot overlaps increase the energy per unit length, producing more liquid and subsequently widening the width of the melt pool. Larger melt pools possess a larger thermal variation across the melt pool and therefore larger surface tension variations. These surface tension variations are subsequently reduced by breaking up the melt pool into spherical molten balls by the balling mechanism, these tend to solidify on the outer edge of the melt pool [Agarwala *et al.* 1995]. Side R_a can be reduced using a high scan speed and low repetition rate (low spot overlap). This encourages quicker melt pool solidification and minimizes the volume of liquid within the melt pool. This produces relatively thin melt pools with less variation in the thermal properties across the melt pool than that of a larger melt pool. The melt pool is more stable and is less likely to suffer from balling.

Figure 5(b) also shows the top and side R_a of each sample produced using 0.5-0.7J pulse energies. The use of higher pulse energies tended to improve both top and side R_a. This is believed to be result of the higher peak powers being generated with the use of higher pulse energies at a fixed pulse duration. High peak powers generate large recoil pressures that exert a mechanical force on the melt pool. Work has shown that larger recoil pressures generated as a result of higher peak powers flatten out the melt pool [Morgan *et al.* 2004] and increase the wettability of the melt [Mumtaz *et al.* 2008]. Improved wettability subsequently reduces a melt pools tendency to undergo balling [Agarwala *et al.* 1995; Kruth *et al.* 2004]. Figure 5(b) shows that minimum top and side R_a are not simultaneously attained due to a variety of factors (volume of liquid produced, surface tension variations, thermocapillary flow) having a tendency to pull these part properties in different directions. The best solution was to compromise on optimum top/side R_a values and settle for values that combined produced the lowest value. The lowest combined top and side R_a was achieved with the use of 0.5ms pulse duration, 0.7J pulse energy, 40Hz repetition rate and 400mm/m scan speed (79.2% spot overlap). This produced a sample with average top R_a 9µm, side R_a 10µm and a wall thickness of 0.49mm. During processing it was observed that a plasma plume reaching 5mm in height was produced, this caused relatively little spatter to settle on the top surface of the powder bed.

Figure 6 shows the standard rectangular pulse shape used in producing the optimized thin wall part. An image of the central portion from the top surface of the thin wall part is also displayed. The average peak power of this pulse was 1.4kW, however the maximum peak power as result of overshoot is 1.8kW. It was observed that overshoot not only occurred with the pulse's power but also with the pulse's duration. Instead of being set at a minimum 0.5ms in duration the pulse extends to 0.7ms, this extension potentially increases the volume of liquid produced and the width of the part.

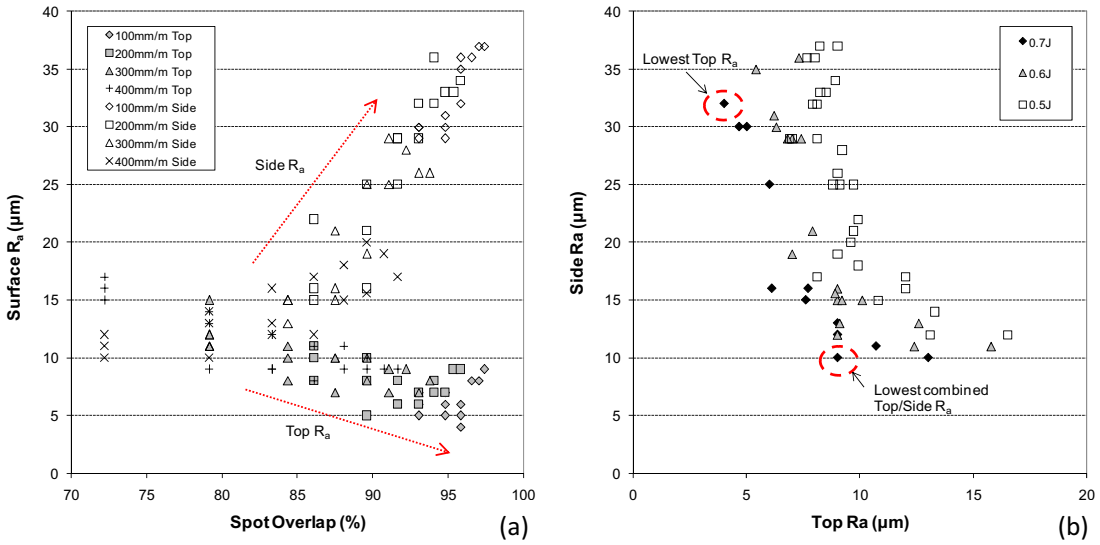

Figure 5 Top/side R_a variation with spot overlap (a) & optimum top/side R_a results (b).

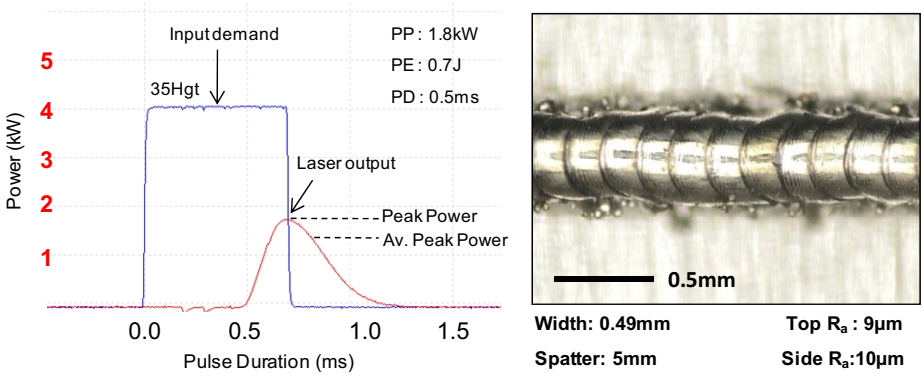

Figure 6 Optimized thin wall sample and standard rectangular pulse shape input and output

4 Pulse shaping Experimentation

During parameter optimization there was difficulty in attaining simultaneously low top and side R_a. It was envisioned that the use of pulse shaping would offer a more precise and tailored control over the heat input and would allow a refining and improvement over current part properties.

4.1 Parameters

Using the repetition rates and scan speeds optimized in section 3.1, a variety of ramp up and ramp down pulse shapes were generated and used to process four layer of Inconel 625 each with a layer thickness of 100µm. The ramp up pulses varied from 1.7ms-10ms and contained pulse energies and peak powers ranging from 0.6-2.2J and 0.7-1kW respectively. Note, it was not possible to produce ramp up pulses shorter than 1.7ms in duration due to nature of pulsed laser generation creating an initial spike at the beginning of the pulse. This

needed to be eliminated in order to allow gradual ramp up power delivery. This was only achieved with extension of the pulse duration above 1.7ms. Ramp down pulses were easier to generate and varied between 1-10ms and contained pulse energies and peak powers ranging from 0.5-2.5J and 1.3-2kW respectively. These range of ramp up and ramp down parameters are shown in Table 2.

Pulse Shape	Pulse Width (ms)	Pulse Energy (J)	Repetition Rate (Hz)	Scan Speed (mm/m)
Ramp Up	1.7-10	0.6-2.2	40	400
Ramp Down	1-10	0.5-2.5	40	400

Table 2 Ramp Up/Down pulse shape processing range

4.2 Pulse Shape Results

Due to the energy distribution within a ramped up pulse shape melt pool generation is more likely to occur at the end of the pulse when peak power is at its highest. Leading up to the main peak power the gradual increase in laser energy heats up the material causing it's reflectivity to drop. As a result of this energy distribution the peak power required to melt Inconel 625 was on average 0.8kW less than that used within a ramped down pulse shape. This ramping up of energy can therefore be viewed as preheating of material, reducing the thermal energy required to achieve full melting (heat balance) and also the amount of spatter generated during processing.

Figure 7 displays top/side R_a of thin walled parts created using the variety of ramp up and ramp down pulses. Trends reveal that top R_a does not vary considerably (9-15µm) with the use of ramp up pulse shapes ranging from 1.7-10ms in duration. Within laser processing of metal powders a lot of energy is required to initiate a melt pool due to high reflectivity. Once the melt pool has been initiated the materials reflectivity drops and subsequently requires less energy to remain molten. The late melt pool formation followed by rapid solidification does not allow surface profile variations to reduce through relaxation mechanisms (movement of fluid due to gravity and surface curvature). This in combination with the use of low peak powers (less recoil pressure) results in a top R_a values that do not vary. Ramp up part side R_a varied more than top R_a (14-42µm) and degraded as pulse duration increased. This is attributed to more liquid being produced with the use of longer pulse durations causing the melt pool width to expand and cause larger thermal variations across the melt pool, promoting balling and increasing side R_a. Due to the use of generally low peak powers with ramp up pulses lower recoil pressure are exerted on the melt pool. As mentioned in section 3.2, larger recoil pressures generated as a result of higher peak powers increase melt pool wettability and suppress balling formation. The lowest combined top/side R_a (10µm and 23µm respectively) was achieved with a 1.7ms ramp up pulse shape using a pulse energy of 0.7J and a peak power of 0.8kW. Due to the low peak power and ramp up energy distribution a minimum level of plasma plume/spatter was generated during processing (1mm in height). As a result of low plasma plume height the negative effects associated with spatter generation during SLM processing would be reduced. This ramp up pulse shape is examined further in section 3.3.

The use of ramp down pulse shapes appears to have a positive effect on top/side R_a with the use of shorter pulse durations (1-2ms). Figure 7 shows that lowest top R_a of 6µm was achieved with a 1.5ms ramp down pulse with 1.1J of pulse energy. This pulse is further examined in section 4.3. Ramp down energy distribution promotes early melt pool formation due to the use of high peak power early within the pulse. This makes the melt pool more prone to expansion as further energy is used to increase the volume of liquid within the melt pool. This promotes the balling mechanism as surface tension variations increase across the melt pool causing side R_a to increase. This is reflected in Figure 7 with ramp down side R_a being generally higher than that of ramp up pulses at similar pulse durations. As with ramp up pulses, increases in ramp down pulse duration increases side R_a.

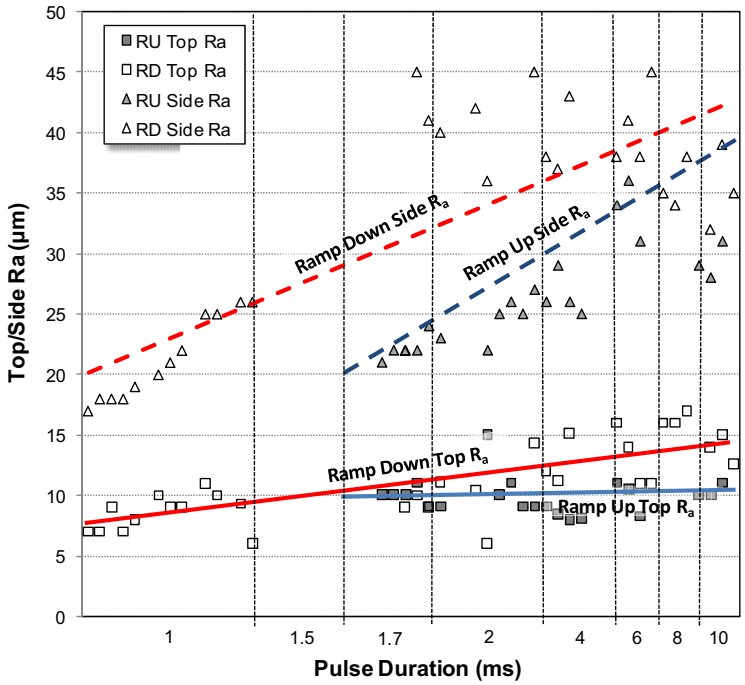

Figure 7 Surface R_a of thin walled part produced using ramp up and ramp down pulse shapes

4.3 Pulse Shape Discussion

Two pulse shapes were identified in section 4.2 to provide benefits during processing of certain part properties compared to those produced using the optimized non pulse shaped standard pulse. Figure 8 displays the standard pulse shape from section 3 along with the two pulse shaped pulses developed in section 4. Each of the pulse shaped pulses has a top surface image of the thin walled produced including a superimposed image of the standard pulse output (used for comparison).

The first effective pulse shape was produced using a ramp up pulse shape. This produced the lowest combined top/side R_a (10µm and 23µm respectively) was achieved using a 1.7ms ramp up pulse shape with a pulse energy of 0.7J and a peak power of 0.8kW. This pulse contained the same amount of energy as the standard optimized pulse yet during

processing produced very little plasma plume/spatter during processing (1mm in height). This is due to the use of a lower peak power and energy distribution gradually introducing heat allowing the materials latent heat of fusion and reflectivity to drop, generating a preheating effect. However due the use of a low peak power (1kW less than the standard optimized pulsed) the side R_a was on average 13µm higher than the standard optimized pulse. As a result of late melt pool initiation the melt pool was small (0.43mm) after not been given enough time to increase its volume. Another possible explanation for low melt pool width could be associated with low peak powers not generating enough recoil pressure to flatten and spread the melt pool and extend its width.

The second effective pulse shape produced the lowest top R_a (6µm) and was achieved using 1.5ms ramp down pulse with a peak power of 1.8kW containing 1.1J of energy. Early melt pool generation, longer laser on time and higher pulse energy allowed more time for capillary and thermo capillary flows to rearrange liquid within the melt pool and reduce variations in the top surface profile of the melt pool. Another possible explanation for low top R_a could be related to reduced melt pool viscosity due to higher attained temperature of melt. Lower viscosity will strengthen any Marangoni convection present within the melt pool assisting the fluid flow and reshaping of melt pool before complete solidification. This pulse contained the same peak power as that of the standard optimized pulse. However due to the increased pulse energy and pulse duration (compared to the standard optimized pulse) the side R_a increased (28µm) as the melt pool widened (0.52mm) promoting the balling mechanism due to increased surface tension variations. Lower viscosity as a result of higher attained temperature of melt can increase melt pools susceptibility to undergo balling [Agarwala *et al.* 1995]. As a result of prolonged pulse duration and increased energy plasma plume reached 6mm in height, visibly increasing the amount of spatter settling on top of the powder bed.

Figure 9 shows the top/side R_a and width of the standard pulse shape and two effective pulse shapes. Ramping up provided no benefit in regard to a reduction in top/side R_a over a non pulse shaped pulse. This is due to the use of low peak powers generating insufficient recoil pressures to modify melt pool shape and inhibit balling formation. However due to low heat input and modified energy distribution, spatter generation during processing was low. This low heat input may also be effective in reducing distortion due to shrinkage and improve the accuracy of parts and help to alleviate mechanical stresses. The ramp down pulse shape measuring 1.5ms in duration was only beneficial in regards to it generating a low top R_a (6µm). The early melt pool generation, prolonged pulse duration and increased pulse energy increased the volume of liquid and widened melt pool width (0.52mm). This increased surface tension variation within the melt pool increasing balling/side R_a. This ramp down pulse would be useful scanning internal geometries of parts but not external side geometries due to high balling formation.

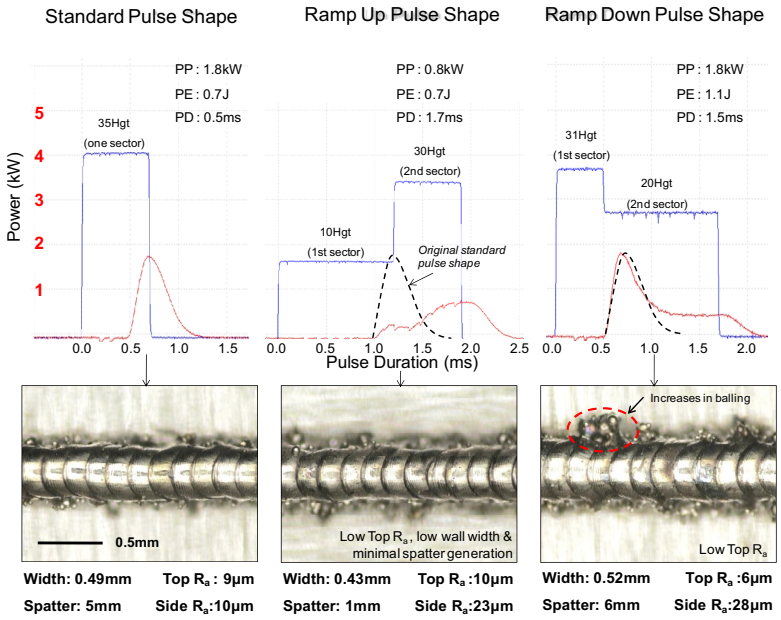

Figure 8 Effective pulse shapes

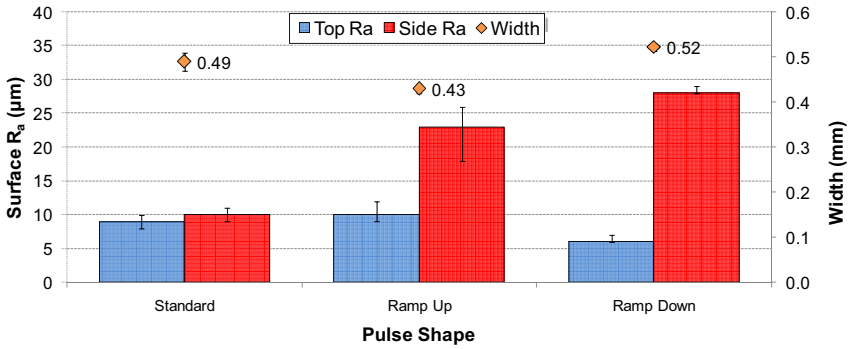

Figure 9 Surface R_a & thickness of parts created using a variety of pulse shapes

5 Conclusions

Optimization experiments discovered that low scan speeds, high repetition rate, high pulse energies, high peak powers (larger spot overlap, higher energy per unit length) reduced top R_a. This was due to reduced variation between overlapping melt pools, reduced melt pool viscosity (increasing strength of Marangoni convection) and delayed melt pool solidification allowing more time for relaxation forces to reshape and modify melt pool surface. Side R_a was reduced using high scan speeds, low repetition rates, high peak powers and lower energy per unit length. This was primarily due to reduced melt pool volume and width reducing the thermal/surface tension variation across the melt pool and inhibiting the balling mechanism. The optimum value for both top/side R_a could not be simultaneously attained due to limited melt pool control as certain factors improved one part characteristic while deteriorating the other.

Pulse shaping experiments were employed in an attempt to further control and refine energy distribution such that wall thickness and R_a could be reduced. Ramp up pulse shapes generally operated at lower peak powers as compared to standard and ramp down pulses. This is because the energy distribution induces a gradual heating of powder particles. The

materials reflectivity dropped as its temperature increased, this reduced the peak power required to induce full melting. The gradual heating could be viewed as pre-heating reducing spatter generation during processing. Ramping up was not effective in reducing top/side R_a due to late melt pool generation and use of low peak powers. Ramp down pulse shapes were able to minimize top R_a due to early melt pool generation, increased pulse duration, increased energy, reduced melt pool viscosity and more time being for capillary and thermocapillary flows to rearrange liquid within the melt pool. However due to the increased heating the volume of liquid present within the melt pool increased causing the melt pool to expand in width. This increase in melt pool width caused a larger variation in thermal properties across the melt pool leading to a larger variation in surface tension, inducing the balling mechanism and increasing side R_a.

SLM is a complex process that imparts large heat intensities within a very short space of time. This rapid heating requires a greater degree of control such that the correct volume of liquid is present within the melt pool and possessing stable qualities (high wettability, low thermal variation across melt pool, low tendency to undergo balling). It has been found that ramping up and ramping down has certain benefits. Side R_a is more difficult to control and tends to degrade at a higher rate than top R_a. Ideally for the production of thin walled parts with combined low top/side R_a a pulse with a high peak power, short pulse durations with low energies should be employed. High peak peaks have been shown to be beneficial in reducing both top and side R_a due to high recoil pressure flattening melt pool and increasing melt pool wettability (suppressing balling mechanism). The shortened pulse generation would permit less time for heat to conduct radially from the centre of the melt pool, reducing the volume of liquid produced within the melt pool and potential for any instability to take place.

6 References

Agarwala, M., D. Bourell, et al. (1995). "Direct selective laser sintering of metals." Rapid Prototyping Journal **1**(1): 26-36.

Badawi, K., M. Paindavoine, et al. (1989). "Effects of spatial and temporal pulse energy distribution of a laser beam on welding " Revue de Métallurgie **86**: 162-170.

Bransch, H. N., D. C. Weckman, et al. (1994). "Effects of Pulse Shaping on Nd:YAG Spot Welds in Austenitic Stainless Steel." Welding Research Supplement(June): 141-151.

Cheng, J., F. Kahlen, et al. (2000). Effects of Intra-Pulse Structure on Hole Geometry In Laser Drilling. ICALEO.

Chichkov, B. N., C. Momma, et al. (1996). "Femtosecond, picosecond and nanosecond laser ablation of solids." Appl Phys A(63): 109-115.

Dalgarno, K. (2007). Materials research to support high performance RM parts. Rapid Manufacturing 2nd International Conference, Loughborough University.

Das, D. K. (1994). "Surface roughness created by laser surface alloying of aluminum with nickel." Surface & Coatings Technology **64**(1): 11.

Fischer, P., V. Romano, et al. (2003). "Sintering of commercially pure titanium powder with a Nd:YAG laser source." Acta Materialia **51**(6): 1651-1662.

Fuh, J. Y. H., Y. S. Choo, et al. (1995). "Improvement of the V curing process for the laser lithography technique." Materials & Design **16**(1): 23-32.

Kanzler, K. (2006). How much energy are you throwing away? Photonics Spectra. **July**.

Katayama, S., S. Kohsaka, et al. (1993). Pulse Shape Optimization for Defect Prevention in Pulsed Laser Welding of Stainless Steels. Proceedings of 12th ICALEO '93, Orlando, Flo.

Kruth, J. P., L. Froyen, et al. (2003). "New ferro powder for selective laser sintering of dense parts." CIRP Annals - Manufacturing Technology **1**(52): 139-142.
Kruth, J. P., L. Froyen, et al. (2004). "Selective laser melting of iron-based powder." Journal of Materials Processing Technology **149**(1-3): 616-622.
Morgan, R., C. J. Sutcliffe, et al. (2004). "Density analysis of direct metal laser re-melted 316L stainless steel cubic primitives." Journal of Materials Science **39**(4): 1195-1205.
Mumtaz, K., N. Hopkinson, et al. (2008). "High Density Selective Laser Melting of Waspaloy." Journal of Material Processing **195**: 77-87.
Niu, H. J. and I. T. H. Chang (1998). "Liquid phase sintering of M3/2 high speed steel by selective laser sintering " Scripta Materialia **30**(1): 67-72.
Park, H. and S. Rhee (1999). "Analysis of mechanism of plasma and spatter in CO2 laser welding of galvanized steel." Optics and Laser Technology **31**(2): 119-126.
Petrov, A. L., A. A. Gusev, et al. (1992). New advances in industry applications of YAG pulse lasers. Proc. LAMP 92.
Ramos, J. A., D. L. Bourell, et al. (2003). Surface over-melt during laser polishing of indirect-SLS metal parts, Boston, MA, United States, Materials Research Society.
Rehme, O. and C. Emmelmann (2005). Reproducibility for properties of Selective Laser Melting products. Proceedings of the Third International WLT-Conference on Lasers in Manufacturing, Munich.
Rombouts, M., J. P. Kruth, et al. (2006). "Fundamentals of Selective Laser Melting of alloyed steel powders." CIRP Annals - Manufacturing Technology **55**(1): 187-192.
Santos, E. C., K. Osakada, et al. (2004). "Microstructure and mechanical properties of pure titanium models fabricated by selective laser melting." Proceedings of the I MECH E Part C Journal of Mechanical Engineering Science **218**(7): 711-719.
Schwendner, K. I., R. Banerjee, et al. (2001). "Direct laser deposition of alloys from elemental powder blends." Scripta Materialia **45**(10): 1123-1129.
Sparks, T., J. Ruan, et al. (2006). Effect of Structured Laser Pulses on Grain Growth in H13 Tool Steel Solid Freeform Fabrication Symposium 2006. Austin, TX.
Weedon, T. M. (1987). Nd:YAG lasers with controlled pulse shape. Proc. LAMP 87.